

Journal Section: Behavioral/systems/Cognitive

Cerebellar Modulation of Trigeminal Reflex Blinks:

Purkinje Cells

Abbreviated Title: Blink-Related Purkinje Cells

Fang-Ping Chen²

Craig Evinger¹

¹Depts. Neurobiology & Behavior and Ophthalmology, SUNY Stony Brook, Stony Brook, NY 11794-5230 ²Dept. Molecular and Cellular Biology, Baylor College of Medicine, One Baylor Plaza BCM130, Houston, TX 77030

Corresponding author:

Craig Evinger

Dept. Neurobiology & Behavior

SUNY Stony Brook

Stony Brook, NY 11794-5230

levinger@notes.cc.sunysb.edu

10 figures

39 pages

Abstract: 251 words

Introduction: 460 words

Discussion: 1,675 words

Keywords: interpositus, blink adaptation, eyelid conditioning

Acknowledgements: We thank Donna Schmidt for her technical assistance. The National Eye Institute supported this work through a grant to CE (EY07391).

ABSTRACT

We identified four regions of Purkinje cells innervating blink-related interpositus neurons, lateral, rostral, dorsal caudal and ventral caudal regions. For all blink-related Purkinje cells, a blink-evoking corneal stimulus evoked a complex spike (CS) followed by a cessation of simple spike (SS) discharge that resumed near the end of eyelid closing. CS latency identified long (>20 ms) and short (<20 ms) latency groups of Purkinje cells. The SS discharge of lateral region Purkinje cells and rostral and dorsal caudal region long CS latency Purkinje cells correlated with trigeminal reflex blinks. The resumption of SS activity after a blink-evoking stimulus correlated with the end of reflex blinks. Changes in the SS firing frequency of these Purkinje cells accounted for the increased blink amplitude and duration during blink adaptation. The SS discharge of short CS latency Purkinje cells in the rostral and dorsal caudal regions and Purkinje cells in the ventral caudal region did not correlate with changes in reflex blinks or during blink adaptation. To determine which regions of physiologically identified Purkinje cells innervated blink-related interpositus pause and burst neurons, we inactivated specific regions while simultaneously recording from interpositus pause neurons. Inactivation of lateral, rostral and dorsal caudal Purkinje cells modified interpositus pause neurons and increased reflex blink amplitude and duration. Inactivation of ventral caudal Purkinje cells, however, did not affect interpositus pause neurons or modify reflex blinks. These data revealed two cerebellar circuits regulating eyelid movements. One modifies trigeminal reflex blinks and supports blink adaptation. The other may support classical eyelid conditioning.

Introduction

The cerebellum is essential for classical eyelid conditioning and blink adaptation and it modulates trigeminal reflex blinks (Evinger et al., 1989; Raymond et al., 1996; Hesslow and Yeo, 1998; Thompson, 2005; Chen and Evinger, 2006). A common assumption about the role of the cerebellum in eyelid motor control and learning is that the same cerebellar circuit modulates all eyelid movements. Studies in humans (Ramnani et al., 2000; Dimitrova et al., 2002; Maschke et al., 2003; Gerwig et al., 2004) and animals (Yeo and Hardiman, 1992; Hesslow, 1994; Hesslow and Yeo, 1998; Yeo, 2004), however, reveal two or three cerebellar cortical regions active with blinking and eyelid conditioning. Although the presence of multiple cortical regions is consistent with a unitary control of all eyelid movements, it could also indicate that independent groups of Purkinje cells modulate different eyelid behaviors. The first interpretation implies that a physiologically homogenous group of interpositus (IP) neurons receives inputs from multiple Purkinje cell regions, whereas the second explanation predicts distinct pools of IP neurons receiving inputs from unique groups of Purkinje cells.

Our previous study (Chen and Evinger, 2006) identified two anatomically and physiologically distinct types of blink related IP neurons. One type, pause neurons, was at the border region between anterior and posterior IP, and the second type, burst neurons, was more rostral in anterior IP. Following corneal stimulation, pause neurons transiently ceased their tonic activity immediately before the end of eyelid closure. The timing of the pause correlated with blink duration and delaying the cessation of tonic activity with gabazine increased the duration of lid closure. In contrast to IP pause neurons, IP burst neurons exhibited a brief cessation of activity followed by increased

activity occurring around the end of eyelid closure in response to a blink-evoking corneal stimulus. Nevertheless, the discharge of IP burst neurons did not correlate with blink duration, and gabazine treatment of these neurons did not modify blink duration. IP pause, but not IP burst, neurons modified their discharge with blink adaptation. Chen & Evinger (2006) suggested that the two groups of IP neurons participated in different forms of cerebellar dependent learning, blink adaptation and eyelid conditioning. Despite similarities between eyelid conditioning and VOR plasticity, a form of adaptation akin to blink adaptation (Raymond et al., 1996), our proposal implied that blink adaptation and eyelid conditioning utilized distinct cerebellar circuits to modify eyelid behavior.

If our proposal is correct, then the two types of blink related IP neurons should receive inputs from distinct pools of Purkinje cells. To test this prediction, we anatomically identify regions of Purkinje cells projecting to blink-related IP neurons, physiologically characterize their discharge patterns during reflex blinking and blink adaptation, and determine the effect of inactivating specific groups of Purkinje cells on IP pause neuron discharge.

Materials and Methods

Experiments were performed on 150-400 g male Sprague-Dawley rats maintained on a 12 hr light/dark cycle and fed ad libitum. All experiments adhered to Federal, State and University guidelines concerning the use of animals in research.

Animals were anesthetized with xylazine (10 mg/kg, im) and urethane (1.2 g/kg in saline, ip) and placed in a stereotaxic apparatus. The skull overlying the cerebellum was removed to allow introduction of microelectrodes. A pair of Teflon coated, stainless steel

wires bared 1 mm at the tip, were implanted into the medial and lateral margins of the upper eyelid to record the orbicularis oculi electromyographic activity (OOemg). In some rats, a 3-0 silk suture was sewn to the center point of the upper eyelid's lower margin to enable lid restraint.

Trigeminal reflex blinks were evoked by electrical corneal stimulation through a pair of silver ball electrodes placed on the cornea. Electrical stimulus intensity was adjusted to produce partial closing of eyelid that did not displace the electrodes. Over all of the experiments, the current intensity necessary to elicit a reliable blink ranged from 0.1 to 3.0 mA using stimulus durations between 100 - 300 μ s. A corneal stimulus was presented on each trial, which occurred every 40 s.

To induce adaptive increases in blink amplitude, the upper eyelid was restrained by connecting the suture attached to the upper eyelid to a fixed bar. The rat received 20 trials before restraint, 40 trials with the eyelid restrained, followed by 40 trials without restraint. Electrical stimulus intensity and placement of the electrodes on the cornea was held constant before, during and after lid restraint. Tears were wicked off of the cornea at the start of the experiment and after every 20th trial.

Single units were recorded extracellularly with a glass micropipette (AM Systems, Carlsborg, WA) filled with 2M NaCl saturated with fast green. Electrode tips were broken to produce impedances between 1 and 4 M Ω to record Purkinje cells. Purkinje cell recording sites were marked with fast green (Thomas and Wilson, 1965). To inactivate specific cerebellar regions and record single IP neurons simultaneously, we used two independent microelectrodes. A double barrel pipette (AM Systems, Carlsborg, WA) was used for lidocaine microinjection into blink related Purkinje cell regions. The

recording barrel of the double barrel electrode was filled with 2M NaCl saturated with fast green, and the other barrel with 2% lidocaine and 10% Evan's blue in saline. A standard glass micropipette was positioned to record blink related IP neurons. After identifying blink-related Purkinje cells, the second electrode was moved to record from a single IP pause neuron. A Picospritzer (General Valve Co., Fairfield, NJ) attached to the lidocaine barrel produced lidocaine microinjections that inactivated the Purkinje cell region. The extent of lidocaine spread was estimated from the spread of Evan's blue and the IP recording site was marked with fast green.

Animals were deeply anesthetized at the end of experiments and perfused transcardially with 6% warm dextran in 0.1M phosphate buffer (PB, pH 7.4), followed by 10% formalin in 0.1M PB. The brains were removed and immersed in 30% sucrose in 0.1M PB for 24 hours. To localize the fast green deposits, 100 μ m sections were cut on a freezing microtome, mounted on subbed slides and counterstained with cresyl violet. In the lidocaine microinjection experiments, slides were counterstained with 2% Neutral Red (Sigma-Aldrich, St. Louis, MO).

Histology

A double barrel electrode glass electrode containing HRP was used to identify Purkinje cells projecting to blink-related IP neurons. The recording barrel was filled with 2M NaCl saturated with fast green, and the other barrel was filled with 15% horseradish peroxidase (HRP, Roche, Nutley, NJ) in distilled water. After identifying blink-related IP neurons with the recording electrode, HRP was iontophoretically injected into the IP region by applying 1-2 μ A of 0.5 Hz square-wave positive current pulses for 10 to 30 minutes. Twenty-four hours later, animals were deeply anesthetized and transcardially

perfused with 6% warm dextran in 0.1M PB, followed by a cold fixative of 1% paraformaldehyde and 1.25% glutaraldehyde in 0.1M PB. The brains were removed and immersed in 30 % sucrose in 0.1M PB. Fifty micron coronal sections were cut on a freezing microtome. Sections were processed with tetramethyl benzidine (TMB, Sigma-Aldrich, St. Louis, MO) method for HRP detection, with β -D-glucose (Sigma-Aldrich, St. Louis, MO) and glucose oxidase (Roche, Nutley, NJ) as the oxygen source for the enzymatic reaction and ammonium molybdate (Sigma-Aldrich, St. Louis, MO) for stabilization (Faulkner et al., 1997). The sections were mounted on slides and counterstained with 2% Neutral Red.

Data collection and analysis

OOemg activity was amplified (AM Systems, Carlsborg, WA, Differential AC Amplifier, model 1700) and filtered from 0.3 to 5 kHz. For all experiments, OOemg and single neuron activity were digitized and collected at 10 kHz per channel (DT2821, Data Translation Marlboro, MA), stored on a personal computer and analyzed off-line with laboratory-developed software. Down phase blink duration was calculated as the time between the start and end of the OOemg activity following a corneal stimulus. Down phase blink amplitude was calculated by integrating the rectified OOemg activity between the beginning and end of the OOemg activity.

Single unit activity was amplified (AM Systems, Carlsborg, WA, Microelectrode AC Amplifier, model 1800) and filtered from 0.3 to 20 kHz. Spikes were identified with a software window discriminator and sorted by template-matching method. For each trial, the tonic firing rate was calculated over the 150 ms before the blink-evoking stimulus.

To allow comparison between neurons and blinks recorded in different experiments, data were normalized to the median of the control data for each recording. An ANOVA was employed to compare the data between populations of neurons or conditions. Regression slopes of different conditions were compared using an analysis of covariance (ANCOVA). All data are presented as the mean \pm standard deviation.

Results

The dorsolateral segments of anterior IP and posterior IP contain blink-related IP burst and pause neurons respectively (Fig. 1A) (Chen and Evinger, 2006). To localize the Purkinje cells projecting to these IP neurons, we injected HRP into the blink-related IP region in five rats (Fig. 1B - D). An injection that covered most of the region containing blink-related IP neurons (Fig. 1B) labeled Purkinje cells in anterior cerebellum, simple lobule, Crus I and II, and paramedian lobule. Based on their locations relative to the blink-related IP region, we divided the cerebellar cortex containing the labeled Purkinje cells into rostral, lateral, dorsal caudal and ventral caudal regions. The rostral region included the rostral part of simple lobule and the lateral portions of lobules V, IV, III and II. The lateral region encompassed portions of sublobule a of Crus I and the caudal end of simple lobule. The caudal regions contained sublobules c and d of Crus I and Crus II (Fig. 1E).

The HRP injections involving only the rostral IP region (Fig. 1C, gray) or the rostral region and some of the posterior region (Fig. 1C, black) indicated that different groups of Purkinje cells innervated the rostral burst and more caudal pause IP neurons (Fig. 1A) (Chen and Evinger, 2006). A small injection in anterior IP primarily involving

burst neurons (Fig.1C, gray) produced more Purkinje cell labeling in the rostral region than in other regions. A few Purkinje cells were also labeled in Crus I d of the caudal region. When the injection site included the entire anterior IP, including rostral pause neurons (Fig. 1C, black), the rostral region, Crus I a of the lateral region, and Crus I c and d of the caudal region contained HRP labeled Purkinje cells. Comparing the location of HRP labeled Purkinje cells among the four cases with the smallest IP injections (Fig. 1C, D) revealed that an injection site restricted to anterior IP primarily labeled Purkinje cells in the rostral and caudal regions. Injections extending further into posterior IP labeled more lateral region Purkinje cells. Given that the posterior pause neurons modulate trigeminal reflex blink duration and amplitude, whereas the rostral burst neurons do not correlate with blink duration (Chen and Evinger, 2006), we predicted that the discharge characteristics of Purkinje cells innervating these two neuronal populations would be different..

We recorded a total of two hundred and eleven Purkinje cells for which a blink-evoking corneal stimulus altered the neuronal discharge. Regardless of location, blink-related Purkinje cells exhibited a similar discharge pattern. The corneal stimulus always elicited a complex spike (CS, Fig 2B, ∇) followed by a transient cessation of simple spike (SS) activity. The neuron then resumed its tonic SS activity or exhibited a transient burst of SS activity (Fig.2B, \downarrow) near the end of OOemg activity (Fig.2B, \uparrow).

Lateral Region

Forty-nine Purkinje cells were recorded in the Crus I a region and two in the caudal end of simple lobule (Fig. 2A). Because these Purkinje cells were likely to be in different microzones (Ivarsson et al., 2002), we sorted Purkinje cells according to their

CS latency (Fig. 2C). Based on this bimodal frequency distribution of CS latencies, we classified Purkinje cells with a CS latency less than 20 ms as short CS latency Purkinje cells (16.73 ± 1.68 ms, $n=19$; Fig. 2A Δ) and neurons with a CS latency greater than 20 ms as long CS latency Purkinje cells (26.5 ± 4.57 ms, $n=32$; Fig. 2A \bullet). In the lateral region, Purkinje cells located superficially tended to have shorter CS latencies than more deeply located Purkinje cells.

Long and short CS latency Purkinje cells shared similar physiological characteristics. The SS tonic firing frequency was not significantly different between the two types of Purkinje cells (short CS latency: 53.2 ± 9.3 ; long CS latency: 55.5 ± 11.8 spikes/sec, $F_{(34)} = 0.35$, $p > 0.05$). For long CS latency Purkinje cells, the first SS action potential after the pause (Fig 2B, \downarrow) began an average of 7.2 ± 21.2 ms ($n = 483$ blinks) after the end of the blink. SS activity began an average of 6.0 ± 19.3 ms ($n=202$ blinks) after the end of the blink for short CS latency neurons. These latencies were not significantly different between the two populations ($F_{(684)} = 0.49$, $p > 0.05$). One difference in SS discharge between long and short CS latency Purkinje cells, however, was that the majority of long CS latency neurons (25 of 32) exhibited a burst of SS activity following the cessation of SS activity (Fig. 2D, black line), whereas only three of nineteen short CS latency neurons showed this burst (Fig. 2D, gray line).

To determine whether the resumption of lateral Purkinje cell SS activity correlated with the end of blink, we averaged the latency of the end of OOemg activity (Fig. 2B \uparrow) relative to the corneal stimulus (Fig. 2B \blacktriangle ; End of Blink Latency) as a function of the latency of the first spike after the pause (Fig. 2B \downarrow) relative to the corneal stimulus (Fig. 2B \blacktriangle ; Simple Spike Latency) for all long ($n= 5-30$ blinks/bin, Fig. 2E, \bullet)

and short CS latency Purkinje cells ($n= 5-13$ blinks/bin, Fig. 2E, Δ). For both groups of Purkinje cells, the end of blink latency increased with the SS latency (Fig. 2E). Because the blink began at a relatively constant time after the corneal stimulus, these data showed that blink duration correlated with SS latency. The regression lines for the long CS latency (slope = 0.45, $r^2=0.74$) and short CS latency Purkinje cells (slope= 0.28, $r^2=0.53$) were not significantly different ($p>0.05$, $F_{(1,50)} = 3.92$).

Rostral Region

Fifty-seven blink-related Purkinje cells were recorded in the rostral region (Fig. 3). The Purkinje cells located in the simple lobules were all short CS latency neurons (16.0 ± 2.1 ms, $n= 14$ neurons, Fig. 3A Δ). With the exception of two short CS latency Purkinje cells located medially in lobule II (Fig. 3A, -9.60 mm), Purkinje cells recorded in lobules V, IV, III, and lateral edges of lobule II were long CS latency neurons (24.8 ± 3.6 ms, $n= 41$ neurons, Fig. 3A \bullet). The SS discharge pattern was similar for the two populations of Purkinje cells. Averaging the simple spike density function for 7 short (Fig. 3B) and 7 long (Fig. 3C) CS latency Purkinje cells and the concomitant OOemg activity revealed there was a pause in SS activity during the OOemg activity that resumed near the end of OOemg activity. There was no significant difference in the SS tonic firing frequency between short and long CS Purkinje cells (short CS latency: 48.1 ± 6.7 spikes/s; long CS latency: 52.9 ± 11.1 spikes/s; $F_{(33)}= 0.98$, $p > 0.05$). The relationship between blink duration and the resumption of SS activity, however, was different for the two groups. There was a concomitant increase in the SS latency and the end of the blink for long CS latency Purkinje cells (slope = 0.41, $r^2 = 0.56$; Fig. 3E), but not for short CS latency Purkinje cells (slope = 0.11, $r^2=0.09$; Fig. 3D). The significant difference in the

slopes of the two regression lines ($F_{(1, 44)} = 6.4$, $p < 0.05$) implied dissimilar roles for the long and short CS latency Purkinje cells in modulating trigeminal reflex blinks.

Dorsal Caudal Region

Blink-related Purkinje cells in the dorsal caudal region were found in Crus I c and the dorsal part of Crus I d (Fig. 4A). Twenty-four short CS latency Purkinje cells (17.5 ± 1.9 ms, Fig. 4A Δ) and thirty-one long CS latency Purkinje cells (24.6 ± 4.1 ms, Fig. 4A \bullet) were recorded in this region. Apart from CS latency, the general pattern of SS discharge was similar for short and long CS latency Purkinje cells. Averaging the simple spike density functions for ten short (Fig. 4B) and ten long (Fig. 4C) CS latency Purkinje cells and the concomitant OOemg activity revealed that the SS discharge ceased during the blink and resumed near the end of OOemg activity. The SS average tonic firing frequency of two groups of Purkinje cells (short CS latency: 43.9 ± 9.6 spikes/s; long CS latency: 43.0 ± 13.6 spikes/s; $F_{(43)} = 0.06$, $p > 0.05$) was not significantly different. The significantly steeper slope ($F_{(1, 57)} = 18.2$, $p < 0.05$) of the regression line relating the SS latency and the end of the blink for long CS latency (slope = 0.32, $r^2 = 0.66$; Fig. 4E) relative to short latency CS Purkinje cells (slope = 0.04, $r^2 = 0.03$; Fig. 4D) showed that reflex blink duration increased with the SS latency for long CS latency Purkinje cells, but not for short CS latency neurons.

Ventral Caudal Region

Five short CS latency Purkinje cells (19.0 ± 0.8 ms, Fig. 5A Δ) and forty-three long CS latency Purkinje cells (26.85 ± 4.5 ms; Fig. 5A \bullet) blink-related Purkinje cells were recorded in the ventral part of Crus I d and Crus II (Fig. 5A). Because there were too few short CS latency Purkinje cells to support a quantitative comparison with long CS

latency neurons, we restricted our analysis to long CS latency Purkinje cells. The SS discharge of the ventral caudal long CS latency Purkinje cells ceased with the blink and resumed their discharge with a burst of activity near the end of the blink (Fig. 5B). This burst activity occurred with the resumption of SS activity for forty-one out of forty-three neurons. The average SS tonic firing frequency was 47.7 ± 10.3 spikes/s ($n=34$). Unlike other blink-related long CS latency Purkinje cells, however, the slope of the linear regression linking the end of blink latency and SS latency was flat (slope = 0.09, $r^2 = 0.1$; Fig. 5C).

Purkinje Cell Activity during Blink Adaptation

Blink duration correlated with the resumption of SS activity for Purkinje cells in the lateral region (Fig. 2E) and long CS latency Purkinje cells in the rostral (Fig. 3E) and dorsal caudal regions (Fig. 4E). We hypothesized that these blink-related Purkinje cells innervated IP pause neurons whose discharge correlated with blink duration (Chen and Evinger, 2006). In contrast, the resumption of SS activity of ventral caudal Purkinje cells (Fig. 5C) and short CS latency rostral (Fig. 3D) and dorsal caudal Purkinje cells (Fig. 4D) did not correlate with reflex blink duration. We hypothesized that these Purkinje cell innervated IP burst neurons. These hypotheses predicted that lateral region Purkinje cells and long CS latency Purkinje cells in the rostral and dorsal caudal regions would modify their SS discharge with blink adaptation as did IP pause neurons, whereas the SS discharge of ventral caudal Purkinje cells and short CS latency rostral and dorsal caudal Purkinje cells would be unaltered as occurred with IP burst neurons (Chen and Evinger, 2006).

Lateral Region Purkinje Cell Activity during Blink Adaptation

For seven of eight experiments with lateral Purkinje cell recordings (five long and two short CS latency neurons), lid restraint significantly increased blink duration by 87% ($F_{(208)} = 17.96$, $p < 0.001$; Fig. 6A) and amplitude by 530% ($F_{(208)} = 38.56$, $p < 0.001$; Fig. 6A). As there was no significant difference of neural activity or blink modifications with lid restraint between short and long CS latency lateral Purkinje cells, we pooled the data from the two groups. For all seven Purkinje cells, lid restraint significantly decreased SS tonic firing frequency by 4% ($F_{(208)} = 4.55$, $p < 0.05$; Fig. 6A, C, TFR). Given that Purkinje cells inhibit IP neurons and IP neurons indirectly excite OO motoneurons through the red nucleus, reducing the tonic firing rate of Purkinje cells should increase blink amplitude. Consistent with a role for lateral Purkinje cells in controlling blink duration, the SS latency occurred 25% later with lid restraint than during the control condition ($F_{(208)} = 20.50$, $p < 0.001$; Fig. 6A, C, SS latency). The CS latency of these Purkinje cells, however, did not change significantly with lid restraint ($F_{(155)} = 0.56$, $p > 0.05$). In the one experiment in which lid restraint failed to increase blink duration and amplitude during the recording, the simultaneously recorded long CS latency Purkinje cell did not alter its SS discharge with lid restraint.

Rostral Region Purkinje Cell Activity during Blink Adaptation

During the recording of eight long CS latency rostral Purkinje cells before and during blink adaptation, lid restraint increased blink duration by 63% ($F_{(182)} = 30.85$, $p < 0.001$; Fig. 6B) and blink amplitude by 246% ($F_{(182)} = 18.94$, $p < 0.001$; Fig. 6B). Long CS latency Purkinje cells significantly modified their discharge pattern in six of these eight experiments. For these six neurons, the SS tonic firing rate significantly decreased

by 7.5% ($F_{(182)} = 5.83$, $p < 0.05$; Fig. 6B, D, TFR,) and there was a significant 25% delay in the SS latency ($F_{(182)} = 40.56$, $p < 0.001$, Fig 6B, D, SS latency). Purkinje cell CS latency did not change significantly with lid restraint ($F_{(115)} = 1.19$, $p > 0.05$). Although lid restraint significantly increased blink duration by 94% ($F_{(48)} = 17.26$, $p < 0.001$) during the other two long CS latency Purkinje cell recordings, the delay in the resumption of SS activity did not change significantly.

Dorsal Caudal Region Purkinje Cell Activity during Blink Adaptation

In nine of ten experiments recording long CS latency Purkinje cells, lid restraint increased blink duration by 152% ($F_{(270)} = 65.86$, $p < 0.001$; Fig. 7A) and blink amplitude by 617% ($F_{(270)} = 65.15$, $p < 0.001$; Fig. 7A). Concomitant with the change in blink amplitude, SS tonic firing rate decreased significantly by 6.5% ($F_{(270)} = 5.69$, $p < 0.05$; Fig. 7A, C, TFR). Concurrent with the increased blink duration, SS latency delayed significantly by 30.1% ($F_{(270)} = 31.86$, $p < 0.001$; Fig. 7A, C, SS latency). CS latency, however, did not change significantly with lid restraint ($F_{(229)} = 1.08$, $p > 0.05$). In the experiment in which blink amplitude and duration did not significantly increase with lid restraint, the SS activity of the long CS latency Purkinje cell recorded during this experiment also did not change.

In contrast to the modified discharge pattern of long CS latency Purkinje cells, SS discharge of two short CS latency Purkinje cells was inappropriate to account for blink adaptation. SS tonic firing frequency was unchanged ($F_{(54)} = .001$, $p > 0.05$) even though lid restraint increased blink amplitude by 510% ($F_{(54)} = 37.35$, $p < 0.001$). Lid restraint shortened SS latency by 14% ($F_{(54)} = 5.29$, $p < 0.05$) even though blink duration

lengthened by 200% ($F_{(54)}=29.5$, $p < 0.001$). There was no significant change in CS latency with lid restraint.

Ventral Caudal Region Purkinje Cell Activity during Blink Adaptation

In six of ten experiments with long CS latency Purkinje cell recordings in the ventral caudal region, blink duration (111%; $F_{(138)} = 21.04$, $p < 0.001$; Fig. 7B) and amplitude (118%; $F_{(138)} = 30.5$, $p < 0.001$; Fig. 7B) increased significantly. Nevertheless, all of the Purkinje cells recorded in these six experiments failed to modify their SS tonic firing frequency (0.9%; $F_{(138)} = 0.039$, $p > 0.05$; Fig. 7B, D, TFR) or lengthen the SS latency significantly (2%; $F_{(138)} = 0.17$, $p > 0.05$; Fig. 7B, D, SS Latency). As in the other experiments, CS latency did not change significantly during lid restraint ($F_{(119)} = 1.03$, $p > 0.05$). For the four experiments in which lid restraint failed to increase the blink amplitude and duration significantly, there were no significant changes in long CS latency Purkinje cell discharge.

Purkinje cell inputs to blink-related IP regions

The data from lid adaptation experiments supported the hypothesis that Purkinje cells in the lateral region and long CS latency Purkinje cells in the rostral and dorsal caudal regions innervated IP pause neurons (Figs. 6, 7). To characterize the role that each type of Purkinje cell might play in controlling the IP pause neuron discharge, the estimated Purkinje cell SS input to IP neurons was compared to the discharge of IP pause neurons using randomly chosen neurons (Fig. 8A). To obtain this estimate, we convolved each SS and CS with a function that approximated that of a unitary postsynaptic IPSP (Traub et al., 2004) using the function:

$$D_{(i)} = (1 - \exp(-t / \alpha)) \exp(-t / \beta)$$

in which $D_{(i)}$ was the estimated synaptic input at time t , α was a 1.45 ms rising rate and β was a 32 ms falling rate. t was incremented every 10 μ s. The result of this convolution was summed over eight trials for five short latency CS lateral, five long CS latency lateral, five long CS latency rostral, and five long CS latency dorsal caudal Purkinje cells. Five IP pause neurons (Chen and Evinger, 2006) were convolved using a double exponential function approximating a unitary EPSP (Sayer et al., 1990) by setting α to 1 ms and β to 20 ms. The five functions for each group of neurons were converted to firing frequency (spikes/s) and averaged. To simplify comparison of Purkinje cell discharge profiles, the tonic firing frequencies of the four Purkinje cell functions were normalized to the short CS latency lateral Purkinje cell function tonic firing frequency in the interval between 73 and 23 ms before the corneal stimulus (Fig. 8, Purkinje cells, red line).

Comparing Purkinje cell (Fig. 8A, top) and IP pause neuron discharge functions (Fig. 8A, bottom) revealed that the short and long CS latency Purkinje cells primarily affected different time windows in the suppression of IP discharge. The CS of the short CS latency lateral Purkinje cells (Fig. 8A, red line \searrow) immediately after the corneal stimulus (Fig. 8A, \blacktriangle) appeared to initiate the suppression of IP activity and the CSs of the long CS latency Purkinje cell types (Fig. 8A, \swarrow) appeared to drive the suppression of IP discharge rapidly to completion. The resumption of short CS latency lateral Purkinje cell SS activity assisted in maintaining suppression of the IP activity (Fig. 8A, Interpositus Activity Suppression). The brief elevation in short CS latency Purkinje cell SS activity should not be able to maintain the prolonged suppression of IP pause neuron activity. The short CS latency lateral Purkinje cell seemed to contribute primarily to the initial suppression of IP pause neuron activity. The maintained suppression of IP activity

appeared to result from the longer latency increase in SS discharge of the long CS latency lateral (Fig. 8A, blue), rostral (Fig. 8A, black), and dorsal caudal (Fig. 8A, green) Purkinje cells. Thus, the CS and SS activity of the short CS latency lateral Purkinje cells appeared to suppress IP pause neuron activity initially, whereas the CS and SS discharge of the long CS latency Purkinje cells seemed to control the longer latency suppression of IP neuron discharge.

To identify the potential roles of long CS latency ventral caudal, short CS latency dorsal caudal, and short CS latency rostral Purkinje cells in modulating the discharge of IP burst neurons, we compared the SS and CS discharge of these groups of Purkinje cells with the discharge of IP burst neurons using the same convolution procedures (Fig. 8B). The transient suppression of IP burst neuron activity following the corneal stimulus was preceded by CSs occurring in short CS latency dorsal caudal and rostral Purkinje cells (Fig. 8B, \blacktriangleleft upper record). The burst of IP burst neuron activity following the brief cessation of activity is consistent with a post inhibitory rebound depolarization (Jahnsen, 1986; Llinas and Muhlethaler, 1988; Aizenman and Linden, 1999, , 2000), coupled with the pause in Purkinje cell SS activity following the CS. The elevated Purkinje cell SS discharge following the cessation in SS activity appears to terminate the burst of IP burst neuron activity. Thus, inputs from long CS latency ventral caudal, short CS latency dorsal caudal, and short CS latency rostral Purkinje cells appear sufficient to explain the IP burst neuron discharge pattern.

To evaluate these proposals further and to identify the relative contribution of the different groups of Purkinje cells to IP discharge pattern, we compared the discharge patterns of an IP pause neuron and concomitant reflex blinks before and after

microinjection of lidocaine at the site of blink-related Purkinje cell recordings. If Purkinje cells in lateral, rostral and dorsal caudal regions innervate IP pause neurons, then inactivating Purkinje cells in these regions should modify IP pause neuron activity and reflex blinks. In contrast, our hypothesis predicted that inactivating blink-related Purkinje cells in the ventral caudal region should not affect IP pause neuron discharge or alter reflex blinks because these Purkinje cells innervate IP burst neurons.

Lateral Region Lidocaine Inactivation

In four experiments, an IP pause neuron was recorded before and after applying lidocaine at the site of blink-related lateral Purkinje cell recordings. To analyze these data, the rectified OOemg activity and the spike density functions of the four IP pause neurons were averaged (Fig. 9A - C). Before lidocaine, the average tonic firing frequency of the four IP pause neurons was 54.5 ± 17.1 spikes/s and the cessation of tonic discharge began 34.9 ± 5.8 ms after the corneal stimulus and lasted 63.1 ± 18.5 ms (Fig. 9A, gray line). Inactivating the lateral Purkinje cell region significantly increased the tonic firing frequency by 17% ($F_{(73)} = 11.85$, $p < 0.005$; Fig. 9A - black line, C, TFR) and significantly delayed the cessation of IP tonic activity by 51.4% ($F_{(73)} = 11.76$, $p < 0.005$; Fig. 9A - black line, C, P Latency). Inactivation reduced the duration of the IP pause suppression by 24.4% ($F_{(73)} = 9.15$, $p < 0.005$; Fig. 9A - black line, C, P Duration) primarily by delaying the start of the pause. As suggested by the Purkinje cell – IP comparison (Fig. 8A), these inactivation data demonstrated that lateral Purkinje cells played a prominent role in producing the initial suppression of IP pause neuron discharge and less of a role in suppressing longer latency IP pause neuron activity.

Concomitant with the delayed onset of the cessation of IP discharge, inactivation of lateral Purkinje cells significantly increased blink duration by 64% ($F_{(73)} = 21.52$, $p < 0.001$; Fig. 10B Δ to \blacktriangledown), similar to the 51.4% delay in the start of the pause in tonic activity (Fig. 9C, P Latency). Consistent with the role of IP pause neurons in modulating the excitability of OO motoneurons, the elevation in IP pause neuron tonic firing frequency produced by lateral region inactivation significantly increased OOemg amplitude (183%, $F_{(73)} = 21.52$, $p < 0.001$).

Rostral Region Lidocaine Inactivation

In three experiments, an IP pause neuron was recorded before and after applying lidocaine at the site of rostral blink-related long CS latency Purkinje cell recordings (Fig. 10D - F). Microinjecting lidocaine into the rostral Purkinje cell region, significantly increased IP pause neuron tonic firing rate by 40.4% ($F_{(61)} = 61.03$, $p < 0.001$; Fig. 10D, F, TFR), delayed the suppression of IP pause neuron activity after the corneal stimulus by 31.6 % ($F_{(61)} = 12.14$, $p < 0.005$; Fig. 9D, F, P Latency), and shortened the duration of the pause in IP neuron discharge by 56.2% ($F_{(61)} = 143.15$, $p < 0.001$; Fig. 9D, F, P Duration). Inactivation of the rostral region caused a significantly larger increase in IP pause neuron tonic firing rate ($F_{(73)} = 21.4$, $p < 0.001$) and reduction in pause duration ($F_{(73)} = 19.1$, $p < 0.001$) than did inactivation of the lateral region. Although lateral inactivation produced a larger delay in the suppression of IP pause neurons than rostral inactivation (Fig. 9), the difference was not significant ($F_{(73)} = 1.6$, $p > 0.05$). As suggested by the Purkinje cell – IP comparison (Fig. 8A), these inactivation data indicated that the long CS latency rostral Purkinje cells played a prominent role in the longer latency components of IP pause neuron suppression.

The delayed onset of the pause and the increase in tonic firing rate of IP pause neuron were accompanied by a 25% increase in OOemg duration ($F_{(61)}=12.0$, $p < 0.05$) and a 128% increase in blink amplitude ($F_{(61)}=10.7$, $p < 0.05$). Although rostral inactivation reduced the duration of the IP pause significantly more than lateral inactivation (Fig. 9), rostral region inactivation increased blink duration less than lateral region inactivation ($F_{(73)} = 11.8$, $p < 0.001$). This apparent incongruity occurred because the onset of the IP suppression is more important in determining blink duration than the duration of the IP suppression (Chen and Evinger, 2003). Lateral inactivation primarily delayed the onset of IP suppression (Fig. 9A, C), whereas rostral inactivation primarily eliminated the later components of the IP suppression (Fig. 9D).

Dorsal Caudal Region Lidocaine Inactivation

In two experiments, an IP pause neuron was recorded before and after applying lidocaine at the site of dorsal caudal Purkinje cell recordings (Fig. 10A-C). Inactivation of the dorsal caudal region slightly elevated IP pause neuron tonic firing frequency (7.9%, $F_{(34)} = 1.31$, $p > 0.05$, Fig. 10C, TFR) and delayed the suppression of IP activity (3%, $F_{(34)} = 0.21$, $p > 0.05$, Fig. 10C, P Latency). Although just missing statistical significance, dorsal caudal inactivation reduced IP pause duration by 17.6% ($F_{(34)} = 3.9$, $p = 0.06$, Fig. 10C, P Duration) primarily by shortening the resumption of IP tonic discharge (Fig. 10A). As suggested by the Purkinje cell – IP comparison (Fig. 8A), these inactivation data supported the hypothesis that the dorsal caudal Purkinje cells modulated the longer latency components of the suppression of IP pause activity. Despite the similarities in the discharge patterns of long CS latency lateral, rostral, and dorsal caudal Purkinje cells (Fig. 8A), the lidocaine microinjections imply that the strength of the

dorsal caudal input onto IP pause neurons was clearly smaller than that of the lateral and rostral Purkinje cells. Consistent with this interpretation, dorsal caudal Purkinje cell inactivation was insufficient to modify either blink duration ($F_{(34)} = 0.13$, $p > 0.05$, Fig.10B) or blink amplitude ($F_{(34)} = 0.014$, $p > 0.05$, Fig.10B) significantly.

Ventral Caudal Region Lidocaine Inactivation

In two experiments, an IP pause neuron was recorded before and after applying lidocaine at the site of ventral caudal Purkinje cell recordings (Fig. 10D - F). As predicted, inactivation of ventral caudal Purkinje cells did not modify the discharge of IP pause neurons. Ventral caudal inactivation increased IP neuron tonic firing frequency by 4.6% ($F_{(26)} = 0.13$, $p > 0.05$; Fig. 10F, TFR) and delayed IP pause neuron suppression by 10.6 % ($F_{(26)} = 0.22$, $p > 0.05$; Fig. 10F, P Latency). In contrast to all of the other inactivation experiments, IP pause duration increased by 4% ($F_{(26)} = 0.09$, $p > 0.05$; Fig. 10F, P Duration). Consistent with the absence of significant changes in IP pause neuron with ventral caudal region inactivation, neither blink amplitude ($F_{(26)} = 0.13$, $p > 0.05$; Fig. 10E) nor blink duration ($F_{(26)} = 0.23$, $p > 0.05$; Fig. 10E) changed significantly.

Discussion

Purkinje Cell Inputs to Blink Related IP Neurons

We identified four regions containing blink-related Purkinje cells: lateral, rostral, dorsal caudal, and ventral caudal regions. Based on their physiological characteristics during reflex blinking and blink adaptation, and the results of lidocaine inactivation, Purkinje cells in those regions appeared to project to either IP pause or IP burst neurons. The data demonstrated that Purkinje cells in the lateral region and long CS latency

Purkinje cells in the rostral and dorsal caudal regions innervated IP pause neurons. The results also indicated that ventral caudal Purkinje cells and the short CS latency Purkinje cells in the rostral and dorsal caudal regions innervated IP burst neurons.

The SS activity of lateral Purkinje cells and long CS latency Purkinje cells in the rostral and dorsal caudal regions correlated with trigeminal reflex blinks. The CS and the resumption of SS discharge following the CS of Purkinje cells assisted in terminating the OO discharge. The inhibition of blink-related IP neurons caused by the Purkinje cell discharge decreased the excitatory drive on OO motoneurons via their red nucleus input (Fanardjian and Manvelyan, 1984; Morcuende et al., 2002; Chen and Evinger, 2006). Consistent with this analysis, blink duration lengthened when the resumption of SS activity was delayed (Figs. 2E, 3E, 4E). Likewise, the delay in the resumption of SS activity and the reduction in tonic firing frequency with lid restraint accompanied the increased blink duration and amplitude (Figs. 6, 7A). The increased reflex blink duration and amplitude caused by inactivation of lateral and rostral Purkinje cells (Fig. 9) demonstrated that the correlation between Purkinje cell discharge and reflex blinks resulted from Purkinje cell actions on blinking through IP pause neurons. Although not achieving statistical significance, the two lidocaine inactivation experiments performed in the dorsal caudal region produced the expected modifications in IP neuron discharge and blink duration (Fig. 10A-C). The small number of inactivation experiments in this region combined with presumed weak influence of these Purkinje cells on IP pause neurons (Fig. 8) probably accounted for the absence of statistically significant changes in the blink. Thus, the anatomical (Fig. 1) and physiological data strongly support the hypothesis that lateral Purkinje cells and long CS latency Purkinje cells in the rostral and

dorsal caudal regions modulate the duration and amplitude of trigeminal reflex blink OO activity through IP pause neurons.

The discharge patterns of lateral Purkinje cells and long CS latency Purkinje cells in the rostral and dorsal caudal regions accounted for IP pause neuron discharge with blinking (Fig. 8A). The initial reduction in IP pause neuron tonic activity resulted from the CS of the short CS latency lateral Purkinje cells. The burst of SS discharge following the cessation activity of long CS latency Purkinje cells maintained the long-lasting suppression of IP pause neurons. During blink adaptation, a blink-evoking stimulus produced a longer than normal cessation of SS activity and delayed the subsequent burst in SS activity for all three groups of Purkinje cells. Despite the absence of a change in CS activity, this prolonged reduction in IP pause neuron inhibition enabled these neurons to remain active longer, thereby lengthening blink duration.

Consistent with innervating IP burst neurons (Chen and Evinger, 2006), the activity of short CS latency Purkinje cells in the rostral and dorsal caudal regions and long CS latency ventral caudal Purkinje cells did not correlate with changes in reflex blink duration or amplitude. Blink termination latency remained constant as the latency of the resumption of SS activity increased following a blink-evoking stimulus (Figs. 3D, 4D, 5C). Long CS latency ventral caudal (Fig. 7B) and short CS latency rostral and dorsal caudal Purkinje cells did not alter their SS or CS discharge with blink adaptation even though reflex blink amplitude and duration increased significantly.

As predicted from our hypothesis that long CS latency ventral caudal Purkinje cells innervated IP burst neurons, inactivating ventral caudal Purkinje cells did not significantly affect IP pause neuron discharge or alter blink amplitude and duration (Fig.

10D-F). Thus, the anatomical (Fig. 1) and physiological data supported the hypothesis that short CS latency Purkinje cells in the rostral and dorsal caudal regions and long CS latency ventral caudal Purkinje cells innervated IP burst, but not IP pause neurons.

The SS and CS timing of short CS latency Purkinje cells in the rostral and dorsal caudal regions and long CS latency ventral caudal Purkinje cells accounted for the discharge pattern of IP burst neurons (Fig. 8B). The CS Purkinje cell discharge explained the initial brief cessation of IP burst neuron activity. This synchronous inhibition could have produced the subsequent burst of IP activity through rebound depolarization (Jahnsen, 1986; Llinas and Muhlethaler, 1988; Aizenman and Linden, 1999, , 2000). The subsequent resumption of Purkinje cell SS activity would have terminated the IP burst.

Parallel Cerebello-olivary Circuits for Eyelid Control

The characteristics of IP pause and burst neurons (Chen and Evinger, 2006) and their distinct Purkinje cell inputs suggest that there are two cerebellar circuits regulating different forms of eyelid behavior. These circuits are distinguishable based on their physiological properties, anatomy, and discharge pattern with blinking.

IP pause and burst neurons appear to possess distinct biophysical properties. The discharge pattern of deep cerebellar neurons (DCNs) ranges from neurons with regular low frequency spontaneous activity that exhibit little rebound depolarization to neurons with a spontaneous bursting pattern for which rebound depolarization evokes a large number of action potentials (Aizenman and Linden, 1999; Aizenman et al., 2003). IP pause neurons fall into the first group. Their average tonic firing frequency (51.2 ± 13.1 spikes/sec) is lower than that of IP burst neurons (64.7 ± 16.95 spikes/s) and IP pause neurons rarely exhibit a burst following the cessation of activity produced by Purkinje

cell input (Chen and Evinger, 2006). DCNs with little rebound depolarization are more likely to exhibit LTD- than LTP-like modifications (Aizenman et al., 1998). The modification of IP Pause neuron activity with lid restraint (Chen and Evinger, 2006) is the change in IP neuron activity expected from an LTD-like modification of the Purkinje cell inhibitory inputs.

Anatomical studies indicate that the C2 zone contains Purkinje cells that receive inputs from the medial accessory olive (MAO) and project to the caudal IP region containing IP pause neurons (Furber and Watson, 1983; Buisseret-Delmas, 1988; Ruigrok and Voogd, 2000; Pijpers et al., 2005). As with the blink-related Purkinje cells in this zone, CS latency in the C2 zone tends to be longer than in the C1/C3 zone (Hesslow, 1994). Thus, a cerebello-olivary circuit composed of the MAO, Purkinje cells in the lateral region, long CS latency Purkinje cells in the rostral and dorsal ventral region and IP pause neurons appears to regulate reflex blinks and blink adaptation on a moment-to-moment basis.

The available data imply that short CS latency Purkinje cells in the rostral and dorsal caudal regions and long CS latency ventral caudal Purkinje cells innervate IP burst neurons to form a second cerebellar circuit that does not regulate reflex blinking or participate in lid adaptation. Based on our data and previous observations, we propose that this cerebellar circuit supports eyelid conditioning. The most effective site for disrupting eyelid conditioning is simple lobule HVI (Yeo et al., 1985a; Attwell et al., 1999; Attwell et al., 2001; Attwell et al., 2002; Freeman et al., 2005), the cerebellar cortex region containing short CS latency rostral Purkinje cells. Other data show that to disrupt eyelid conditioning completely, it is necessary to also block Crus I and II (Yeo

and Hardiman, 1992; Freeman et al., 2005), regions containing ventral and dorsal caudal Purkinje cells. Blocking the anterior IP, the primary location of IP burst neurons (Fig. 1A)(Chen and Evinger, 2006) disrupts eyelid conditioning in rabbits and rodents (Yeo et al., 1985b; Ramnani and Yeo, 1996; Nolan et al., 2002; Freeman et al., 2005; Ohyama et al., 2006). Consistent with our physiological data indicating that short CS latency Purkinje cells in the rostral and dorsal caudal regions and long CS latency ventral caudal Purkinje cells innervate IP burst neurons, anatomical studies demonstrate projections from these cortical regions to the anterior IP (Yeo et al., 1985c; Buisseret-Delmas, 1988; Steinmetz et al., 1992), the location of IP burst neurons (Fig. 1A).

Inferior olive projections to the rostral and dorsal caudal regions containing short CS latency Purkinje cells and the ventral caudal region containing long CS latency Purkinje cells further support the role of this cerebellar cortex – IP burst neuron circuit in eyelid conditioning. The dorsal accessory olive (DAO) appears to be critical in eyelid conditioning (Mauk et al., 1986; Yeo et al., 1986; Medina et al., 2002) and provides short latency inputs to the cerebellar cortex (Hesslow, 1994). In the current study, most of the Purkinje cells identified as innervating IP burst neurons exhibit short CS latency responses to blink-evoking corneal stimuli. Finally, the C1/C3 zones, which project to anterior IP and receive inputs from the DAO (Lang et al., 1999; Ruigrok and Voogd, 2000; Pijpers et al., 2005), include the Purkinje cells projecting to IP burst neurons. Thus, the evidence support a cerebello-olivary circuit involved in eyelid conditioning, the DAO innervating short CS latency Purkinje cells in the rostral and dorsal caudal regions and ventral caudal Purkinje cells that project to IP burst neurons.

Our data and existing evidence support the hypothesis that there are two cerebello-olivary circuits controlling eyelid movements. One circuit composed of the MAO, Purkinje cells in the lateral, long CS latency rostral and dorsal caudal region, and IP pause neurons regulate reflex blinking and blink adaptation. The second circuit, DAO – short CS latency rostral and dorsal caudal, and long CS latency ventral caudal Purkinje cells – IP burst neurons, appear to support eyelid conditioning. The presence of two parallel, functionally distinct cerebellar circuits accounts for the discrepant observations concerning the role of the cerebellum in eyelid conditioning and reflex blinks (Welsh and Harvey, 1989; Steinmetz et al., 1992; Welsh, 1992) and provide a physiological basis for the distinctly different kinematics of blinking and conditioned eyelid movements (Gruart et al., 1995; Powers et al., 2000; Koekkoek et al., 2005).

References

- Aizenman CD, Linden DJ (1999) Regulation of the rebound depolarization and spontaneous firing patterns of deep nuclear neurons in slices of rat cerebellum. *J Neurophysiol* 82:1697-1709.
- Aizenman CD, Linden DJ (2000) Rapid, synaptically driven increases in the intrinsic excitability of cerebellar deep nuclear neurons. *Nat Neurosci* 3:109-111.
- Aizenman CD, Manis PB, Linden DJ (1998) Polarity of long-term synaptic gain change is related to postsynaptic spike firing at a cerebellar inhibitory synapse. *Neuron* 21:827-835.
- Aizenman CD, Huang EJ, Linden DJ (2003) Morphological correlates of intrinsic electrical excitability in neurons of the deep cerebellar nuclei. *J Neurophysiol* 89:1738-1747.
- Attwell PJ, Rahman S, Yeo CH (2001) Acquisition of eyeblink conditioning is critically dependent on normal function in cerebellar cortical lobule HVI. *J Neurosci* 21:5715-5722.
- Attwell PJ, Rahman S, Ivarsson M, Yeo CH (1999) Cerebellar cortical AMPA-kainate receptor blockade prevents performance of classically conditioned nictitating membrane responses. *J Neurosci* 19:RC45.
- Attwell PJ, Ivarsson M, Millar L, Yeo CH (2002) Cerebellar mechanisms in eyeblink conditioning. *Ann N Y Acad Sci* 978:79-92.
- Buisseret-Delmas C (1988) Sagittal organization of the olivocerebellonuclear pathway in the rat. II. Connections with the nucleus interpositus. *Neurosci Res* 5:494-512.
- Chen F-P, Evinger C (2003) Two functions of blink-related interpositus neurons. *Society Neuroscience Abstracts* 29:391.398.
- Chen FP, Evinger C (2006) Cerebellar modulation of trigeminal reflex blinks: interpositus neurons. *J Neurosci* 26:10569-10576.
- Dimitrova A, Weber J, Maschke M, Elles HG, Kolb FP, Forsting M, Diener HC, Timmann D (2002) Eyeblink-related areas in human cerebellum as shown by fMRI. *Hum Brain Mapp* 17:100-115.
- Evinger C, Pellegrini JJ, Manning KA (1989) Adaptive gain modification of the blink reflex. A model system for investigating the physiologic bases of motor learning. *Ann N Y Acad Sci* 563:87-100.
- Fanardjian VV, Manvelyan LR (1984) Peculiarities of cerebellar excitation of facial nucleus motoneurons. *Neurosci Lett* 49:265-270.
- Faulkner B, Brown TH, Evinger C (1997) Identification and characterization of rat orbicularis oculi motoneurons using confocal laser scanning microscopy. *Exp Brain Res* 116:10-19.
- Freeman JH, Jr., Halverson HE, Poremba A (2005) Differential effects of cerebellar inactivation on eyeblink conditioned excitation and inhibition. *J Neurosci* 25:889-895.
- Furber SE, Watson CR (1983) Organization of the olivocerebellar projection in the rat. *Brain Behav Evol* 22:132-152.
- Gerwig M, Dimitrova A, Maschke M, Kolb FP, Forsting M, Timmann D (2004) Amplitude changes of unconditioned eyeblink responses in patients with cerebellar lesions. *Exp Brain Res* 155:341-351.

- Gruart A, Blazquez P, Delgado-Garcia JM (1995) Kinematics of spontaneous, reflex, and conditioned eyelid movements in the alert cat. *J Neurophysiol* 74:226-248.
- Hesslow G (1994) Correspondence between climbing fibre input and motor output in eyeblink-related areas in cat cerebellar cortex. *J Physiol* 476:229-244.
- Hesslow G, Yeo C (1998) Cerebellum and learning: a complex problem. *Science* 280:1817-1819.
- Ivarsson M, Millar L, Yeo C (2002) Electrophysiological Mapping of Eyeblink Microzones in the Rabbit. *Annals of the New York Academy of Sciences* 978:1.
- Jahnsen H (1986) Electrophysiological characteristics of neurones in the guinea-pig deep cerebellar nuclei in vitro. *J Physiol* 372:129-147.
- Koekkoek SK, Yamaguchi K, Milojkovic BA, Dortland BR, Ruigrok TJ, Maex R, De Graaf W, Smit AE, VanderWerf F, Bakker CE, Willemsen R, Ikeda T, Kakizawa S, Onodera K, Nelson DL, Mientjes E, Joosten M, De Schutter E, Oostra BA, Ito M, De Zeeuw CI (2005) Deletion of FMR1 in Purkinje cells enhances parallel fiber LTD, enlarges spines, and attenuates cerebellar eyelid conditioning in Fragile X syndrome. *Neuron* 47:339-352.
- Lang EJ, Sugihara I, Welsh JP, Llinas R (1999) Patterns of spontaneous purkinje cell complex spike activity in the awake rat. *J Neurosci* 19:2728-2739.
- Llinas R, Muhlethaler M (1988) Electrophysiology of guinea-pig cerebellar nuclear cells in the in vitro brain stem-cerebellar preparation. *J Physiol* 404:241-258.
- Maschke M, Erichsen M, Drepper J, Jentzen W, Muller SP, Kolb FP, Diener HC, Timmann D (2003) Cerebellar representation of the eyeblink response as revealed by PET. *Neuroreport* 14:1371-1374.
- Mauk MD, Steinmetz JE, Thompson RF (1986) Classical conditioning using stimulation of the inferior olive as the unconditioned stimulus. *Proc Natl Acad Sci U S A* 83:5349-5353.
- Medina JF, Nores WL, Mauk MD (2002) Inhibition of climbing fibres is a signal for the extinction of conditioned eyelid responses. *Nature* 416:330-333.
- Morcuende S, Delgado-Garcia JM, Ugolini G (2002) Neuronal premotor networks involved in eyelid responses: retrograde transneuronal tracing with rabies virus from the orbicularis oculi muscle in the rat. *J Neurosci* 22:8808-8818.
- Nolan BC, Nicholson DA, Freeman JH, Jr. (2002) Blockade of GABAA receptors in the interpositus nucleus modulates expression of conditioned excitation but not conditioned inhibition of the eyeblink response. *Integr Physiol Behav Sci* 37:293-310.
- Ohshima T, Nores WL, Medina JF, Riusech FA, Mauk MD (2006) Learning-induced plasticity in deep cerebellar nucleus. *J Neurosci* 26:12656-12663.
- Paxinos G, Watson C (2005) *The Rat Brain In Stereotaxic Coordinates*, fifth Edition. San Diego: Academic Press.
- Pijpers A, Voogd J, Ruigrok TJ (2005) Topography of olivo-cortico-nuclear modules in the intermediate cerebellum of the rat. *J Comp Neurol* 492:193-213.
- Powers AS, Coburn-Litvak PS, Evinger C (2000) A conditioned blink is not a blink. *Society for Neuroscience Abstracts* 26:1993.
- Ramrani N, Yeo CH (1996) Reversible inactivations of the cerebellum prevent the extinction of conditioned nictitating membrane responses in rabbits. *J Physiol* 495 (Pt 1):159-168.

- Ramnani N, Toni I, Josephs O, Ashburner J, Passingham RE (2000) Learning- and expectation-related changes in the human brain during motor learning. *J Neurophysiol* 84:3026-3035.
- Raymond JL, Lisberger SG, Mauk MD (1996) The cerebellum: a neuronal learning machine? *Science* 272:1126-1131.
- Ruigrok TJ, Voogd J (2000) Organization of projections from the inferior olive to the cerebellar nuclei in the rat. *J Comp Neurol* 426:209-228.
- Sayer RJ, Friedlander MJ, Redman SJ (1990) The time course and amplitude of EPSPs evoked at synapses between pairs of CA3/CA1 neurons in the hippocampal slice. *J Neurosci* 10:826-836.
- Steinmetz JE, Lavond DG, Ivkovich D, Logan CG, Thompson RF (1992) Disruption of classical eyelid conditioning after cerebellar lesions: damage to a memory trace system or a simple performance deficit? *J Neurosci* 12:4403-4426.
- Thomas RC, Wilson VJ (1965) Precise localization of Renshaw cells with a new marking technique. *Nature* 206:211-213.
- Thompson RF (2005) In search of memory traces. *Annu Rev Psychol* 56:1-23.
- Traub RD, Bibbig A, LeBeau FE, Buhl EH, Whittington MA (2004) Cellular mechanisms of neuronal population oscillations in the hippocampus in vitro. *Annu Rev Neurosci* 27:247-278.
- Welsh JP (1992) Changes in the motor pattern of learned and unlearned responses following cerebellar lesions: a kinematic analysis of the nictitating membrane reflex. *Neuroscience* 47:1-19.
- Welsh JP, Harvey JA (1989) Cerebellar lesions and the nictitating membrane reflex: performance deficits of the conditioned and unconditioned response. *J Neurosci* 9:299-311.
- Yeo CH (2004) Memory and the cerebellum. *Curr Neurol Neurosci Rep* 4:87-89.
- Yeo CH, Hardiman MJ (1992) Cerebellar cortex and eyeblink conditioning: a reexamination. *Exp Brain Res* 88:623-638.
- Yeo CH, Hardiman MJ, Glickstein M (1985a) Classical conditioning of the nictitating membrane response of the rabbit. II. Lesions of the cerebellar cortex. *Exp Brain Res* 60:99-113.
- Yeo CH, Hardiman MJ, Glickstein M (1985b) Classical conditioning of the nictitating membrane response of the rabbit. I. Lesions of the cerebellar nuclei. *Exp Brain Res* 60:87-98.
- Yeo CH, Hardiman MJ, Glickstein M (1985c) Classical conditioning of the nictitating membrane response of the rabbit. III. Connections of cerebellar lobule HVI. *Exp Brain Res* 60:114-126.
- Yeo CH, Hardiman MJ, Glickstein M (1986) Classical conditioning of the nictitating membrane response of the rabbit. IV. Lesions of the inferior olive. *Exp Brain Res* 63:81-92.

Figure Legends

Figure 1. HRP injections into the blink-related interpositus (IP) area. (A) The location of blink-related IP pause (shaded square) and burst (filled circles) neurons (Chen and Evinger, 2006) on coronal rat deep cerebellar nuclei schematics (Ruigrok and Voogd, 2000) separated by 160 μm . (B), (C), (D) The locations of HRP injection sites. Each shaded area shows the extent of one injection. (E) The location of HRP labeled Purkinje cells from the injection illustrated in B plotted on schematic sections of the rat cerebellum (Paxinos and Watson, 2005) Each dot shows the location of a labeled cell in the Purkinje cell layer. Abbreviations: 1,2,3,4,5,6, cerebellar lobules; 4V, 4th ventricle; AIP, anterior interpositus; Cop, copula of the pyramis; Crus 1, crus1 of the ansiform lobule; Crus 2, crus2 of the ansiform lobule; DLH, dorsolateral hump; DLP, dorsolateral protuberance; DN, Dentate nucleus; Fl, flocculus; FN, fastigial nucleus; icf, intercrural fissure; icp, inferior cerebellar peduncle; LVN, lateral vestibular nucleus; mcp, middle cerebellar peduncle; pcuf, preculminate fissure; PFl, paraflocculus; pfs, parafloccular sulcus; PIP, posterior interpositus; plf, posterolateral fissure; PM, paramedian lobule; ppf, prepyramidal fissure; prf, primary fissure; psf, posterior superior fissure; scp, superior cerebellar peduncle; Sim, simple lobule; SimA, simple lobule A; SimB, simple lobule B; simf, simplex fissure.

Figure 2. Characteristics of lateral region Purkinje cells. (A) Recording sites of blink-related Purkinje cells with CS latency shorter than 20 ms (Δ), blink-related Purkinje cells with CS latency greater than 20 ms (\bullet), and unrelated Purkinje cells (\times). (B) Single trial of blink-related long CS latency Purkinje cell activity (top) and concomitant rectified OOemg activity (bottom) evoked by a corneal stimulus (\blacktriangle). The end of blink OOemg

activity (\uparrow) occurs near the resumption of SS activity (\downarrow) following the complex spike (∇). (C) Bimodal frequency distribution of CS latencies for Purkinje cells recorded in the lateral region. (D) The upper records are the averaged SS density functions of seven short (gray line) CS latency and seven long (black line) CS latency Purkinje cells. The lower records are averages of the concomitant OOemg activity elicited by corneal stimulation (\blacktriangle) collected during these Purkinje cell recordings. (E) The latency of the end of OOemg activity relative to the corneal stimulus (End of Blink Latency) as a function of the latency of the resumption of simple spike activity (Simple Spike Latency) relative to corneal stimulation for Purkinje cells with short (\triangle) and long (\bullet) complex spike latency. Each point is the average of 5-30 trials in 2 ms bins of SS latency. The solid line shows the linear regression for data points from long CS latency Purkinje cells and the dashed line the linear regression for data points from short CS latency Purkinje cells. Abbreviations: 5,6,10, cerebellar lobules; Crus1a, crus 1 a of the ansiform lobule; Crus 1b, crus 1b of the ansiform lobule; PFl, paraflocculus; pfs, parafloccular sulcus; prf, primary fissure; psf, posterior superior fissure; Sim, Simple lobule; simf, simplex fissure. Brain schematics from Paxinos and Watson (2005).

Figure 3. Characteristics of rostral region Purkinje cells. (A) Recording sites of rostral region blink-related short (\triangle) and long (\bullet) CS latency Purkinje cells. (B) The upper record is the averaged simple spike density function of seven short CS latency Purkinje cells. The lower record is the averaged concomitant OOemg activity evoked by corneal stimulation (\blacktriangle). (C) The upper record is the averaged simple spike density function of seven long CS latency Purkinje cells. The lower record is the averaged concomitant OOemg activity evoked by corneal stimulation (\blacktriangle). (D) The end of OOemg activity

latency (End of Blink Latency) as a function of the latency of the resumption of SS activity (Simple Spike Latency) relative to corneal stimulation for short CS latency Purkinje cells. Each point is the average of 11-36 trials in 2 ms bins of SS latency. The solid line is the linear regression for these data points. (E) The end of OOemg activity latency (End of Blink Latency) as a function of the latency of the resumption of SS activity (Simple Spike Latency) relative to corneal stimulation for long CS latency Purkinje cells. Each point is the average of 4-20 trials in 2 ms bins of SS latency. The solid line is the linear regression for these data points. Abbreviations: 1,2,3,4,5, cerebellar lobules; Crus1a, crus 1 a of the ansiform lobule; Fl, flocculus; icp, inferior cerebellar peduncle; mcp, middle cerebellar peduncle; pcuf, preculminate fissure; PFl, paraflocculus; prf, primary fissure; scp, superior cerebellar peduncle; Sima, simple lobule A; Simb, simple lobule B. Brain schematics from Paxinos and Watson (2005).

Figure 4. Characteristics of dorsal caudal region Purkinje cells. (A) Recording sites of blink-related short (Δ) and long (\bullet) CS latency Purkinje cells in the dorsal caudal region. (B) The upper record is the averaged SS density function of seven short CS latency Purkinje cells. The lower record is the averaged concomitant OOemg activity elicited by corneal stimulation (\blacktriangle). (C) The upper record is the averaged SS density function of seven long CS latency Purkinje cells. The lower record is the averaged concomitant OOemg activity elicited by corneal stimulation (\blacktriangle). (D) The end of OOemg activity latency (End of Blink Latency) as a function of the latency of the resumption of SS activity (Simple Spike Latency) relative to corneal stimulation for short CS latency Purkinje cells. Each point is the average of 5-21 trials in 2 ms bins of SS latency. The solid line is the linear regression for these data points. (E) The end of OOemg activity

latency (End of Blink Latency) as a function of the latency of the resumption of SS activity (Simple Spike Latency) relative to corneal stimulation for long CS latency Purkinje cells. Each point is the average of 9-29 trials in 2 ms bins of simple spike latency. The solid line is the linear regression for these data points. Abbreviations: 6,7,8,9,10, cerebellar lobules; Cop, copula of pyramis; Crus1c, crus 1 c of the ansiform lobule; Crus1d, crus 1 d of the ansiform lobule; Crus 2, crus 2 of the ansiform lobule; icf, intercrural fissure; PFl, paraflocculus; plf, posterolateral fissure; PM, paramedian lobule; ppf, prepyramidal fissure; psf, posterior superior fissure; sf, secondary fissure. Brain schematics from Paxinos and Watson (2005).

Figure 5. Characteristics of ventral caudal region Purkinje cells. (A) Recording sites of blink-related short (Δ) and long (\bullet) complex spike latency and unrelated (\times) Purkinje cells in the dorsal caudal region. (B) The upper record is the averaged SS function of ten long CS latency Purkinje cells. The lower record is the averaged concomitant OOemg activity evoked by corneal stimulation (\blacktriangle). (C) The end of OOemg activity latency (End of Blink Latency) as a function of the latency of the resumption of SS activity (Simple Spike Latency) relative to corneal stimulation for long CS latency Purkinje cells. Each point is the average of 4-25 trials in 2 ms bins of simple spike latency. The solid line is the linear regression for these data points. Abbreviations: 6,7,8,9,10, cerebellar lobules; Cop, copula of pyramis; Crus1c, crus 1 c of the ansiform lobule; Crus1d, crus 1 d of the ansiform lobule; Crus 2, crus 2 of the ansiform lobule; icf, intercrural fissure; PFl, paraflocculus; plf, posterolateral fissure; PM, paramedian lobule; ppf, prepyramidal fissure; psf, posterior superior fissure; sf, secondary fissure. Brain schematics from Paxinos and Watson (2005).

Figure 6. Lateral and rostral region Purkinje cell discharge during blink adaptation. (A) The upper record is the averaged SS density functions of seven lateral region Purkinje cells (five long and two short CS latency Purkinje cells) before (gray line, Control) and during (black line, Restrained) eyelid restraint. The lower record is the averaged concomitant OOemg activity elicited by corneal stimulation (▲) before (gray line) and during (black line) eyelid restraint. (B) The upper record is the averaged SS density functions of six rostral region long CS latency Purkinje cells before (gray line, Control) and during (black line, Restrained) eyelid restraint. The lower record is the averaged concomitant OOemg activity elicited by corneal stimulation (▲) before (gray line) and during (black line) eyelid restraint. (C) For lateral Purkinje cells, the tonic firing frequency (TFR), latency of the onset of SS resumption (SS Latency) before (black bar) and during (hatched bar) eyelid restraint. (D) For rostral Purkinje cells, the tonic firing frequency (TFR), latency of the onset of simple spike resumption (SS Latency) before (black bar) and during (hatched bar) eyelid restraint. *, $p < 0.05$; **, $p < 0.01$; ***, $p < 0.001$

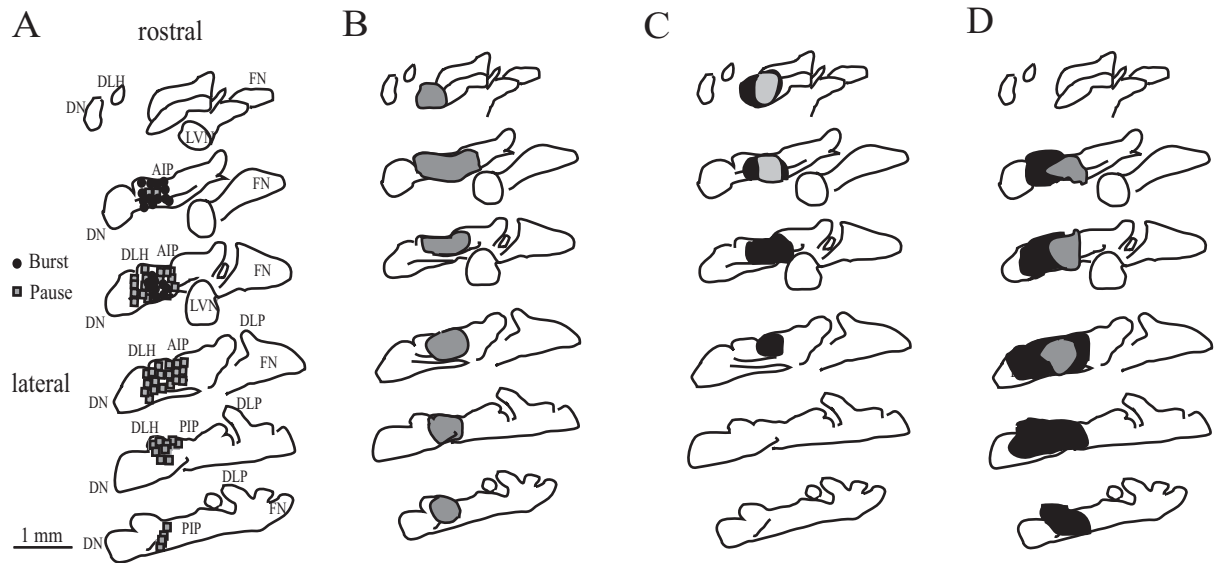
Figure 7. Dorsal caudal and ventral caudal region Purkinje cell activity during blink adaptation. (A) The upper record is the averaged SS density functions of nine dorsal caudal region long CS latency Purkinje cells before (gray line, Control) and during (black line, Restrained) eyelid restraint. The lower record is the averaged concomitant OOemg activity evoked by corneal stimulation (▲) before (gray line) and during (black line) eyelid restraint. (B) The upper record is the averaged SS density functions of six ventral caudal region long CS latency Purkinje cells in before (gray line, Control) and during (black line, Restrained) eyelid restraint. The lower record is the averaged concomitant

OOemg activity evoked by corneal stimulation (\blacktriangle) before (gray line) and during (black line) eyelid restraint. (C) For dorsal caudal Purkinje cells, the tonic firing frequency (TFR), latency of the onset of the resumption of SS activity (SS Latency) before (black bar) and during (hatched bar) eyelid restraint. (D) For ventral caudal Purkinje cells, the tonic firing frequency (TFR), latency of the onset of SS resumption (SS Latency) before (black bar) and during (hatched bar) eyelid restraint. **, $p < 0.01$; ***, $p < 0.001$.

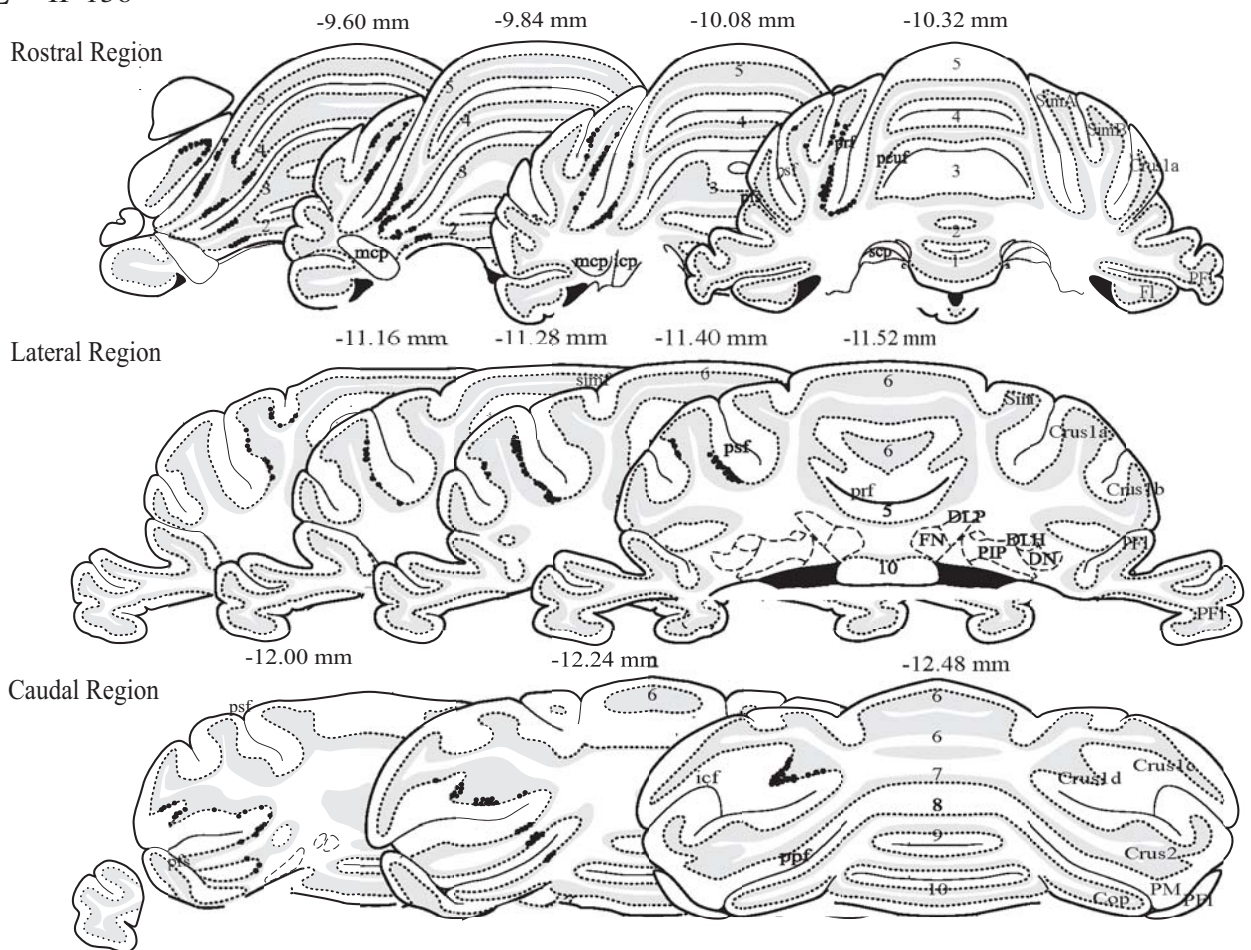
Figure 8. Comparison of the simple and complex spike discharge pattern of blink-related Purkinje cells with the discharge pattern of blink-related interpositus neurons. (A) Top records: The averaged spike density functions of complex and simple spikes from five short CS latency lateral (red), five long CS latency lateral (blue), five long CS latency rostral (black), and five long CS latency dorsal caudal (green) Purkinje cells following a blink-evoking corneal stimulus (\blacktriangle). Arrows show the occurrence of complex spikes. Bottom record: The averaged spike density functions of five interpositus pause neurons following a blink-evoking corneal stimulus (Chen and Evinger, 2006). Horizontal dashed lines show the average tonic firing frequency before the corneal stimulus. (B) Top records: The averaged spike density functions of simple and complex spikes from five long CS latency ventral caudal (brown), five short CS latency dorsal caudal (green), and five short CS latency rostral (black) Purkinje cells following a blink-evoking corneal stimulus (\blacktriangle). Arrows show the occurrence of complex spikes. Bottom record: The averaged spike density functions of five interpositus burst neurons (Chen and Evinger, 2006). Horizontal dashed lines show the average tonic firing frequency before the corneal stimulus.

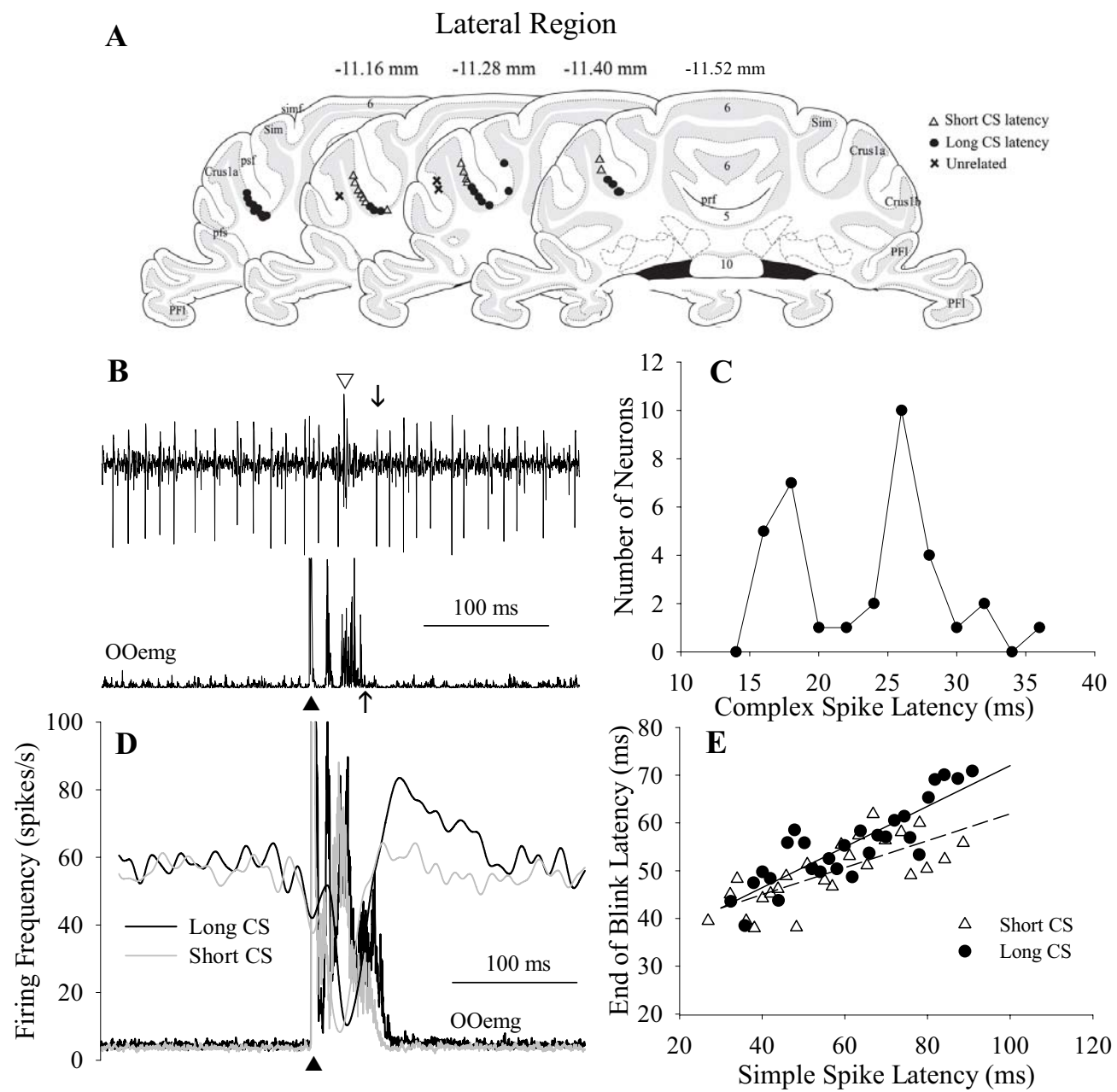
Figure 9. Effects of microinjecting lidocaine at the site of lateral and rostral Purkinje cell recordings on interpositus pause neuron activity and reflex blinks. (A) The averaged spike density functions of four IP pause neurons with corneal stimulation (▲, vertical line) before (gray line) and after (black line) microinjecting 2% lidocaine at the site of lateral region blink-related Purkinje cell recordings. (B) The averaged concomitant OOemg activity evoked by corneal stimulation (▲) before (gray line) and after (black line) lidocaine microinjection at the site of lateral region blink-related Purkinje cells recordings. The end of blink after lidocaine (▼) occurred after the end of the blink on trials before lidocaine (△). (C) Tonic firing frequency (TFR), latency of the suppression of interpositus pause neuron activity (P Latency), and the duration of the suppression of interpositus pause neuron activity (P Duration) before (black bar) and after (hatched bar) lidocaine microinjection at the site of lateral region blink-related Purkinje cell recordings. (D) The averaged spike density functions of three IP pause neurons with corneal stimulation (▲, vertical line) before (gray line) and after (black line) microinjecting 2% lidocaine at the site of rostral region blink-related Purkinje cell recordings. (E) The averaged concomitant OOemg activity evoked by corneal stimulation (▲) before (gray line) and after (black line) lidocaine microinjection at the site of rostral region blink-related Purkinje cells recordings. The end of blink after lidocaine (▼) occurs after the end of the blink before lidocaine (△). (F) Tonic firing frequency (TFR), latency of the suppression of interpositus pause neuron activity (P Latency), and the duration of the suppression of interpositus pause neuron activity (P Duration) before (black bar) and after (hatched bar) lidocaine microinjection at the site of rostral region blink-related Purkinje cell recordings. **, $p < 0.01$; ***, $p < 0.001$

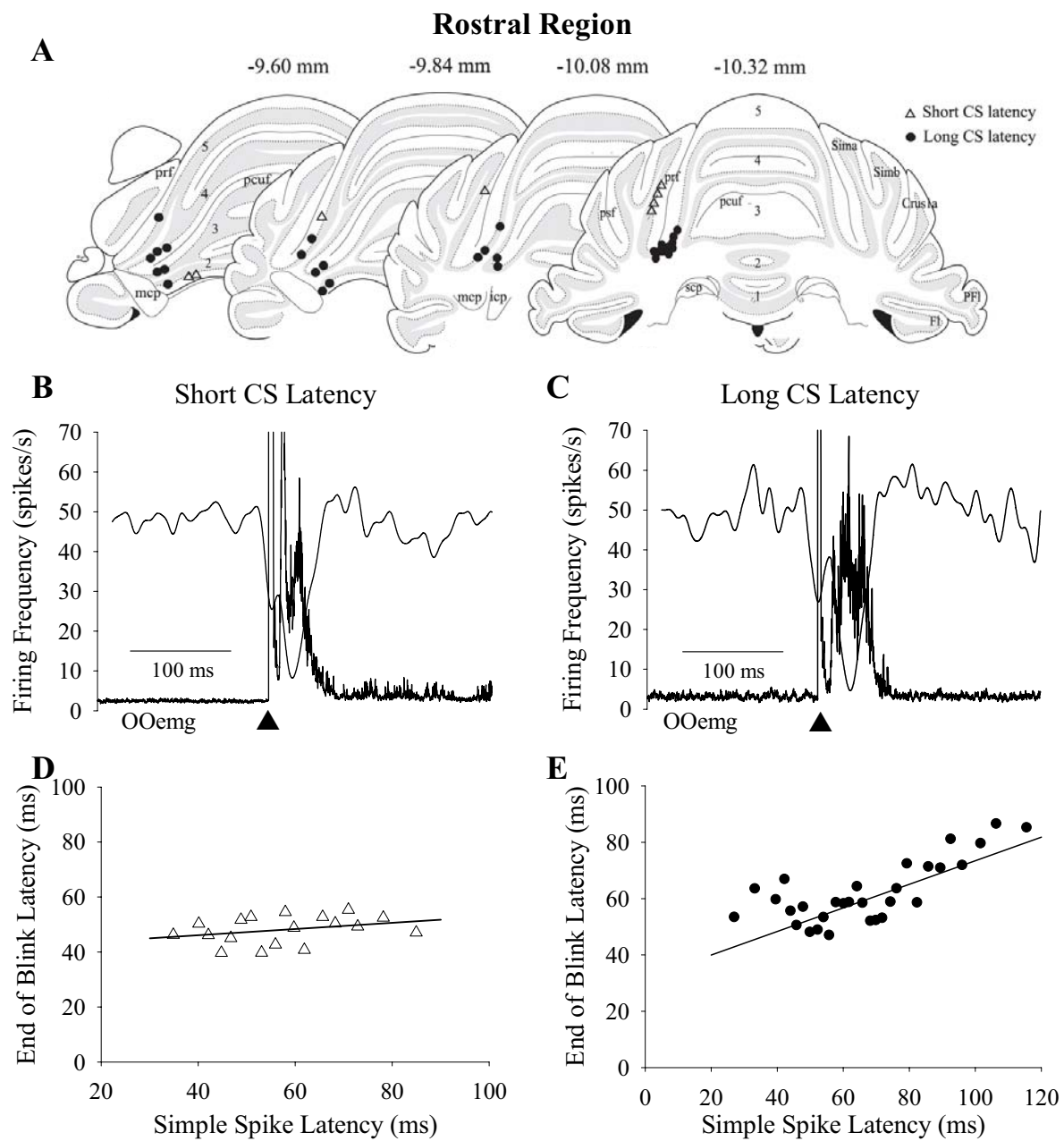
Figure 10. Effects of microinjecting lidocaine at the site of dorsal caudal and ventral caudal Purkinje cell recordings on IP pause neuron activity and reflex blinks. (A) The averaged spike density functions of two IP pause neurons in response to corneal stimulation (▲, vertical line) before (gray line) and after (black line) microinjecting 2% lidocaine at the site of dorsal caudal region blink-related Purkinje cell recordings. (B) The averaged concomitant OOemg activity elicited by corneal stimulation (▲) before (gray line) and after (black line) lidocaine microinjection at the site of dorsal caudal region blink-related Purkinje cells. △ indicates the end of blink before lidocaine, ▼ shows the end of blink after lidocaine. (C) Tonic firing frequency (TFR), latency of the suppression of interpositus pause neuron activity (P Latency), and the duration of the suppression (P Duration) of IP pause neuron activity before (black bar) and after (hatched bar) lidocaine microinjection at the site of dorsal caudal Purkinje cell recordings. (D) The averaged spike density functions of three IP pause neurons in response to corneal stimulation (▲, vertical line) before (gray line) and after (black line) microinjecting 2% lidocaine at the site of ventral caudal region blink-related Purkinje cell recordings. (E) The averaged concomitant OOemg activity evoked by corneal stimulation (▲) before (gray line) and after (black line) lidocaine microinjection at the site of blink-related Purkinje cells in the ventral caudal region. △ indicates the end of blink before lidocaine, ▼ indicates the end of blink after lidocaine. (F) Tonic firing frequency (TFR), latency of the suppression of IP pause neuron activity (P Latency), and the duration of the suppression of IP pause neuron activity (P Duration) before (black bar) and after (hatched bar) lidocaine microinjection at the site of ventral caudal Purkinje cell recordings.

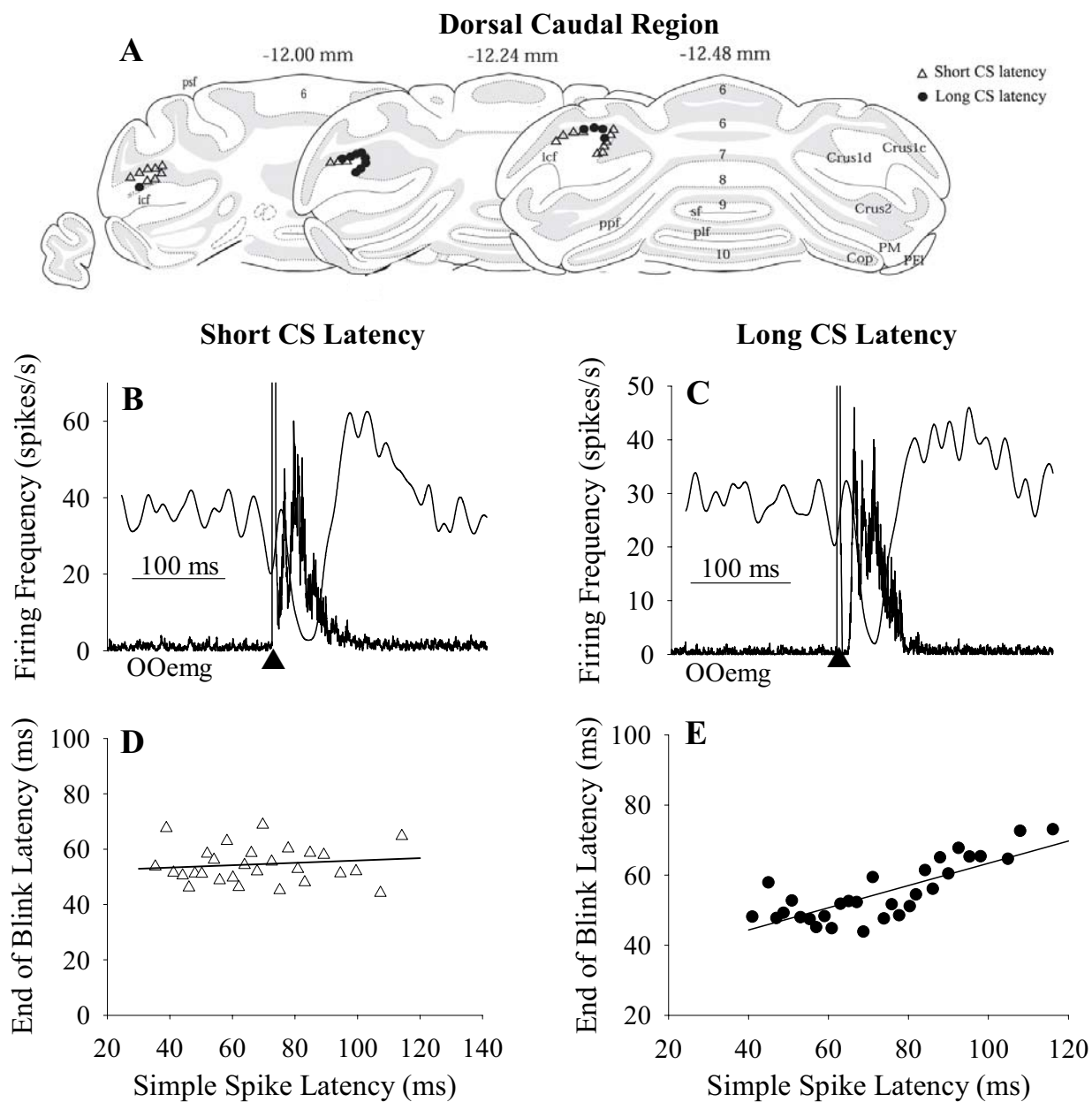


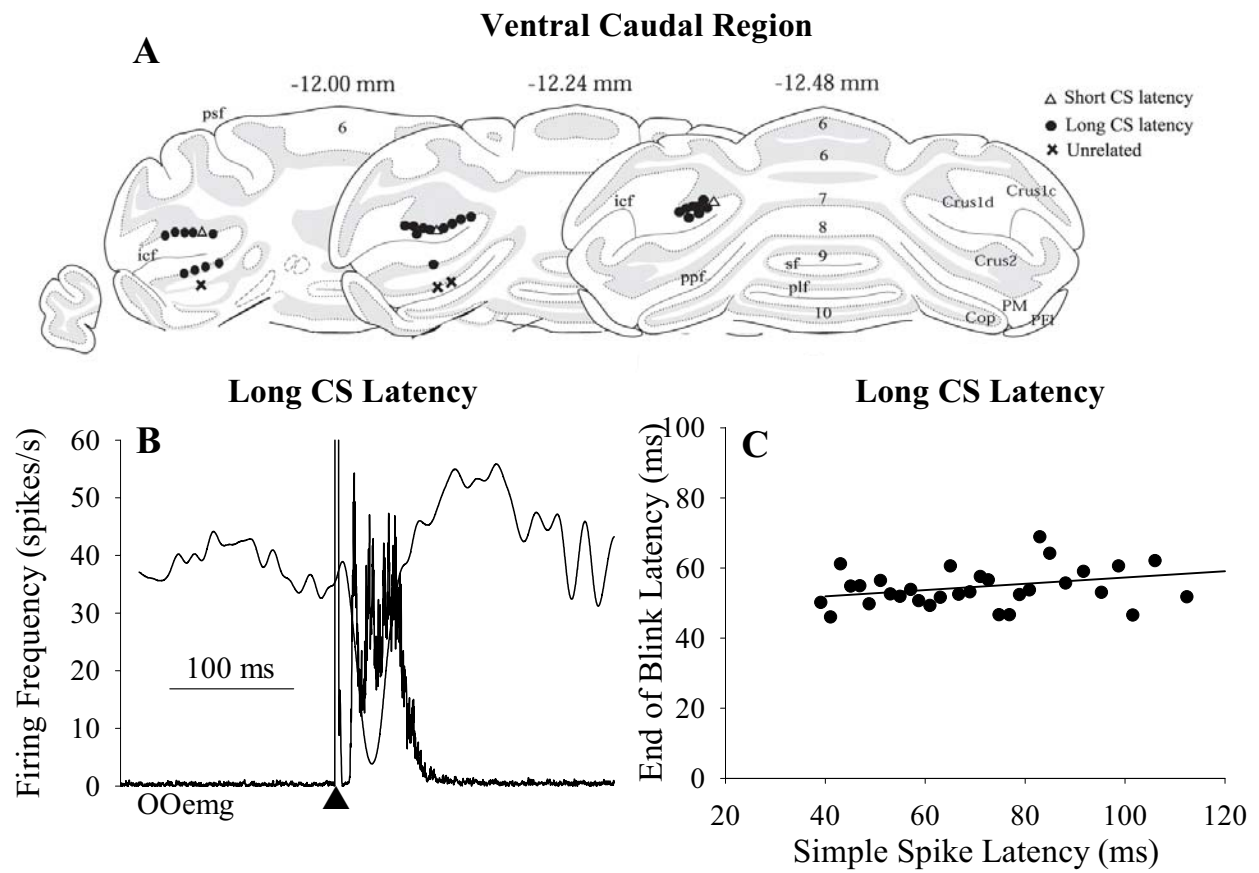
E IP 156

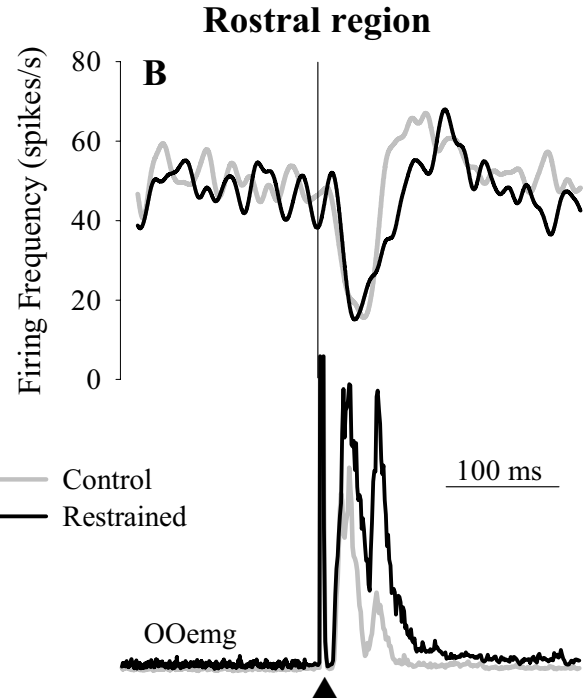
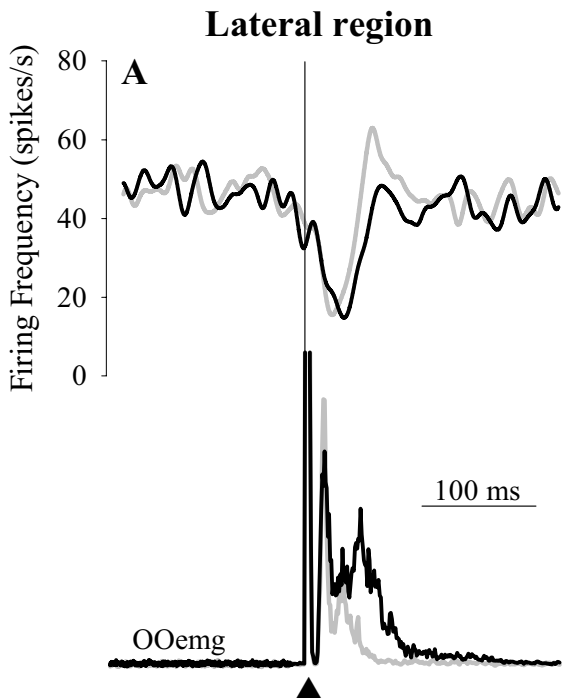












— Control
— Restrained

